Int. J. Electrochem. Sci., 12 **(2017)** 4597 – 4609, doi: 10.20964/2017.05.25

International Journal of
ELECTROCHEMICAL
SCIENCE
www.electrochemsci.org

Carbon Nanofibers Decorated with Pt-Co Alloy Nanoparticles as Catalysts for Electrochemical Cell Applications. I. Synthesis and Structural Characterization

Roxana Muntean[1,2], *Dragoș-Toader Pascal*[1,2], *Gabriela Mărginean*[2], *Nicolae Vaszilcsin*[1,*]

[1] Faculty of Industrial Chemistry and Environmental Engineering, Politehnica University Timișoara, 300006 Piața Victoriei 2, Timișoara, Romania
[2] Department of Materials Science and Testing, Westphalian University of Applied Sciences, Neidenburger Str. 4345897, Gelsenkirchen, Germany
[*]E-mail: nicolae.vaszilcsin@upt.ro

Received: 7 September 2016 / *Accepted:* 17 February 2017 / *Published:* 12 April 2017

Pt-Co alloy deposition on carbon nanofibers (CNF) is achieved using an electrochemical method: pulsed plating current technique. In order to improve the hydrophilic properties of fibers, to achieve a better dispersion of the catalyst particles, CNF were previously functionalized using oxygen plasma treatment. The optimization of the deposition parameters has been performed by linear and cyclic voltammetry, varying the concentration ratio between Pt^{2+} and Co^{2+} in the electrolyte. Obtained samples were characterized using scanning electron microscopy combined with energy dispersive X-ray spectroscopy in respect to their structure and chemical composition, as well as X-ray diffraction for Pt-Co alloy phase identification. The amount of catalyst found onto the substrate material after the deposition process has been determined using thermogravimetric analyses and the Pt-Co ratios in the alloy were checked with X-ray fluorescence spectroscopy. The electrochemical surface area was measured using cyclic voltammograms plotted in H_2SO_4 0.5 M solution. It was found that, employing this electrochemical method and applying the selected deposition parameters, beside the pure Pt particles, a rich Pt-Co alloy phase is formed, namely $CoPt_3$. The amount of $CoPt_3$ varies with the increase of Co content in the deposition bath. The obtained electrodes show a high surface area which may be attributed to structural changes achieved by alloying process, combined with the large surface area of the CNF employed as support.

Keywords: Pt-Co electrodeposition, Carbon nanofibers, Oxygen plasma activation, Electrocatalysts

1. INTRODUCTION

In the last period, several methods and techniques have been developed in order to obtain materials with increased catalytic properties for electrochemical devices, water electrolysis as well as

for proton exchange membrane fuel cells (PEMFC). Studies have revealed that platinum is the metal with the highest catalytic activity [1]. The most frequent strategies applied in order to improve the catalyst activity are either based on support materials with increased surface area, or catalyst deposition with reduced particle sizes, both leading to an increased active surface area [2]. For commercial applications, it is necessary to develop affordable catalyst materials with high performances and stability in the desired working conditions. Carbon-based support materials, with an increased surface area, exhibit a great interest in this field. Lately, a significant number of studies related to platinum deposition onto this type of materials have proved that platinum alloyed with different transitional metals like Co, Fe, Cr, Ni, offers an increased catalytic activity [3, 4] towards the oxygen reduction reaction, even superior than pure platinum, reducing significantly the production costs [5, 6]. Numerous studies regarding this direction have confirmed the performance of Pt-Co alloys for the cathodic reaction inside a fuel cell. It is considered that this alloy improves the durability and in the same time reduces the migration and dissolution of platinum that occur during fuel cell operation [7, 8]. Pt-Co alloys can be deposited onto several support materials by employing various methods. The most frequently used deposition methods are impregnation [5, 9, 10], microemulsion [11], redox transmetallation reactions [12], or electrochemical method [6, 7]. In comparison with other deposition methods, the electrochemical technique presents several advantages. Among these, it is very important to mention the improvement of electrical contact between catalyst particles and support material. This aspect has a strong influence on the catalytic activity of the obtained material. Furthermore, the utilization degree of the catalyst material is significantly increased and the process is simple and cost-effective [13].

In normal conditions, it is difficult to obtain a Pt-Co alloy employing the electrodeposition method from a simple salt electrolyte. Analysing the redox potential values of these two metals, one can observe that platinum deposits faster than cobalt, which is a less noble metal. It has been reported that when complexing agents are added in the deposition bath, an anomalous codeposition process can occur, case in which cobalt deposits preferentially [7, 8]. Moreover, during the deposition process, when high current densities are reached, the hydrogen evolution reaction (HER) takes place. Considering that platinum deposition occurs at more positive potential values, once the current density increase, the platinum concentration at the electrolyte/electrode interface decreases and the deposition process is mass-transfer limited. When the electrode potential is shifted to more negative values, the cobalt deposition can occur simultaneously with the HER [7]. At higher negative potentials, correlated with small pH values, the dominant cathodic reaction is the HER. If the H_3O^+ concentration in the electrolyte is limited, HER is diffusion limited. When the Pt-Co deposition is carried by applying a pulsed plating technique, the deposition and the HER can be easily controlled by adjusting the pulse amplitude (t_{on}), as well as the applied current density (i). One of the most important factors that strongly influences the cathodic Pt-Co codeposition is the specific surface area of the working electrode. Consequently, the current density deposition is likely to be chosen in respect to the surface area, as a higher surface require a higher applied current density. Moreover, the Pt^{2+}/Co^{2+} ratio from the deposition bath can be adjusted in order to facilitate the alloy deposition. A higher cobalt concentration in the electrolyte has a favourable effect on the Pt-Co alloy amount [13]. By applying the pulsed current technique, the compensation of the metal ions from the electrode/electrolyte interface,

consumed during the deposition process is re-established during the pause time (t_{off}). Consequently, a longer t_{off} between pulses is recommended in order to achieve the initial concentration of metallic ions in the solution.

The present study aims to investigate the possibility to obtain Pt-Co alloy catalysts with low platinum loading, suitable for electrochemical cell applications, using an electrochemical method, from a free-additive electrolyte bath. The co-deposition of Pt and Co is achieved by applying a pulsed current technique, varying the Pt^{2+}/Co^{2+} concentration ratios in the electrolyte. The high electrochemical surface area is reached by employing oxygen-plasma treated CNF as support material and moreover, the applied deposition parameters are chosen in order to generate small catalyst alloy particles with a great distribution onto the support material.

2. EXPERIMENTAL

2.1. CNF functionalization

CNF with a high graphitization degree (up to 100%), high specific surface area of about 105-115 $m^2 g^{-1}$ and small diameter, type S-VGCF have been employed as support material for Pt-Co catalyst deposition. Firstly, the CNF were functionalized using radio-frequency oxygen plasma treatment, then the fibers were mixed with isopropanol (99% purity, Carl Roth), and finally the obtained ink was manually sprayed onto a gas diffusion layer (GDL) support material, commercially available (Freudenberg H2315 I2C6). The functionalization treatment was performed in order to increase the hydrophilic properties of the fibers for achieving a better dispersion and also to facilitate the deposition process of the catalyst particles. A great advantage of the plasma functionalization treatment is the easy control of the process correlated with a short exposure time required in order to achieve a proper functionalization degree. In comparison with other functionalization treatments, this method is clean and eco-friendly since no toxic by-products are released in the atmosphere during the operation. The functional groups (carbonyl, carboxyl, hydroxyl) created onto the carbon structures subjected to plasma treatment process provide active sites for catalyst particles, subsequently increasing the deposition rate.

The plasma treatment has been performed using a low-pressure plasma reactor (Plasma Finish RFG 300 RF) which operates at normal temperatures, by applying 80 W power during a period of 1800 s. The plasma parameters for the functionalization treatment of CNF were optimized in a previous work [14]. After the functionalization step, the CNF were mixed with isopropanol (5 mg/10 mL) and ultrasonicated for 15 min in order to achieve a homogenous dispersion. The resulted ink was sprayed onto the GDL support material (25 cm^2) by successive applications, then dried in an oven at 80°C in order to obtain a uniform CNF layer with a 5 μm thickness and a loading of about 0.2 mg cm^{-2}. For electrochemical investigations, the samples have been cut into disks with a diameter of 15 mm.

2.2. Optimization of Pt-Co electrodeposition process

In order to have a general overview of the Pt-Co alloy electrodeposition and for a better understanding of the deposition mechanism, linear and cyclic voltammetry measurements have been performed. For this purpose, 5 different deposition baths have been prepared by maintaining constant the Pt concentration (5 mM) and varying the Co concentration (2.5 mM, 5 mM, 10 mM, 25 mM, and 50 mM). In order to study the individual Pt and Co deposition, two baths containing 0.1 M Co and 5 mM Pt, respectively are also prepared. The solutions are formulated using distilled water and all the chemicals (K_2PtCl_4, $CoCl_2$, H_3BO_3, KCl) are used with no additional purifying process (Sigma Aldrich, Germany). The electrochemical measurements were carried out with the aid of a potentiostat/galvanostat Ivium Technologies Vertex, at room temperature, in a three-electrode cell, with a Saturated Calomel Electrode (SCE) serving as reference and a platinum disk as counter-electrode.

2.3. Pt-Co alloy electrodeposition on CNF

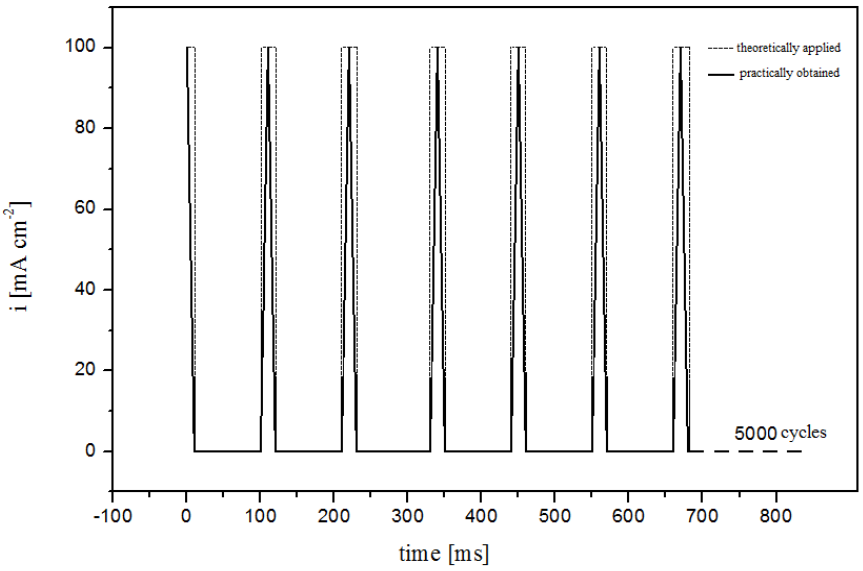

Figure 1. Schematic representation of *i* - *t* plots for Pt-Co deposition process: *i* = 100 mA cm^{-2}, t_{on} = 20 ms, t_{off} = 100 ms, 5000 cycles.

The Pt-Co alloy deposition was carried out galvanostatically on the CNF surface, using the same configuration employed for the electrochemical measurements, in a two-electrode cell, by applying current pulses. The geometric surface of the working electrode was 1 cm^2. Using this method, the current distribution is improved and the obtained alloy deposit consists in particles with a uniform distribution onto the CNF surface. Size of the catalyst particles and chemical composition can be easily controlled by adjusting the deposition parameters as t_{on}, t_{off}, as well as the current density *i*. Several values for the current density were applied in order to detect the optimum value; t_{on} was varied from 10 ms to 20 ms and the number of pulses was changed in respect to the desired catalyst amount. The

working parameters have been chosen in order to achieve an optimal catalyst amount and distribution. The Pt-Co electrodes referred in this work are obtained applying 100 mA cm^{-2} current density, 20 ms for t_{on}, 100 ms for t_{off}, during 5000 cycles. Fig. 1 schematically emphasizes the parameters of the applied deposition process.

2.4. Characterization of the obtained catalyst materials

The morphology and structure of the CNF samples decorated with Pt-Co alloy nanoparticles are investigated using SEM combined with EDX using a Philips XL 30 ESEM Microscope equipped with an EDX detector. Employing this technique, the average size of the deposited catalyst particles can be determined. The crystallographic structures of the prepared samples, as well as the Pt-Co alloy phase are identified using XRD. The measurements are conducted with the aid of an X-Ray Diffractometer (X'Pert MPD System, Philips). This device offers the possibility to identify and analyse with a high resolution, pure materials, as well as alloys and mixtures. The measurements are based on the crystalline or polycrystalline structure of the materials. Appling this method, it was possible to determine and quantify the alloy phases obtained in this study. The data was acquired by scanning the sample at a 2θ angle in the range of 20° and 100°, with a scan rate of 5° min^{-1} at 45 kV and 40 mA.

To determine the catalyst amount deposited onto the CNF support material, thermogravimetric measurements were carried out using a Netzsch STA 449 F1 instrument. The samples, previously dried at 80°C to remove the adsorbed humidity, having an initial weight of around 23 mg, were fixed in an Al_2O_3 crucible and heated with a constant rate from 30°C up to 1200°C in synthetic-air atmosphere. When the maximum temperature was achieved, the system has been maintained in isothermal conditions for 30 min in order to assure a complete burning of the flammable components. The rest mass corresponds to the metallic catalyst particles related to 1 cm^2 sample.

Electrochemical properties and catalytic activity have been evaluated by cyclic voltammetry (CV). Measurements were performed in 0.5 M H_2SO_4 solution, using the previously described electrochemical cell configuration. The working electrode consisted in freshly prepared Pt-Co samples. The CVs are plotted by scanning the potential from -200 mV to 800 mV, with 100 mV s^{-1} scan rate. The solution is purged with nitrogen for 30 min before each experiment. This method offers the possibility to determine the electrochemical surface area (*ECSA*) values of the catalysts, by calculating the necessary charge for H_2 adsorption process.

3. RESULTS AND DISCUSSION

3.1. Linear voltammetry for Pt-Co deposition process

Fig. 2 presents linear voltammograms for the deposition process of Co, Pt and Pt-Co alloy respectively. The measurements were performed in the cathodic region, starting from the electrode potential of 0 V vs. SCE up to -1 V/SCE, with a scan rate of 5 mV s^{-1}. Deposition of Pt and Co takes place according to equations (1) and (2) [15]:

$PtCl_4^{2-} + 2e^- \rightarrow Pt + 4Cl^-$ ($E° = 0.43$ V vs. SCE) (1)

$Co^{2+} + 2e^- \rightarrow Co$ ($E° = -0.52$ V vs. SCE) (2)

The voltammogram for Co deposition shows a low cathodic current density up to about -0.5 V, due to the reduction of oxygen containing groups from the CNF surface. It can be assigned that at more negative potentials, cobalt deposition starts with a considerable overpotential. When the potential reaches more negative values (-0.9 V), the current density is significantly increased and the cobalt deposition process occurs simultaneously with the hydrogen evolution reaction. For platinum deposition, the process starts at more positive potential values, and at -0.3 V the current density increases due to the hydrogen evolution reaction.

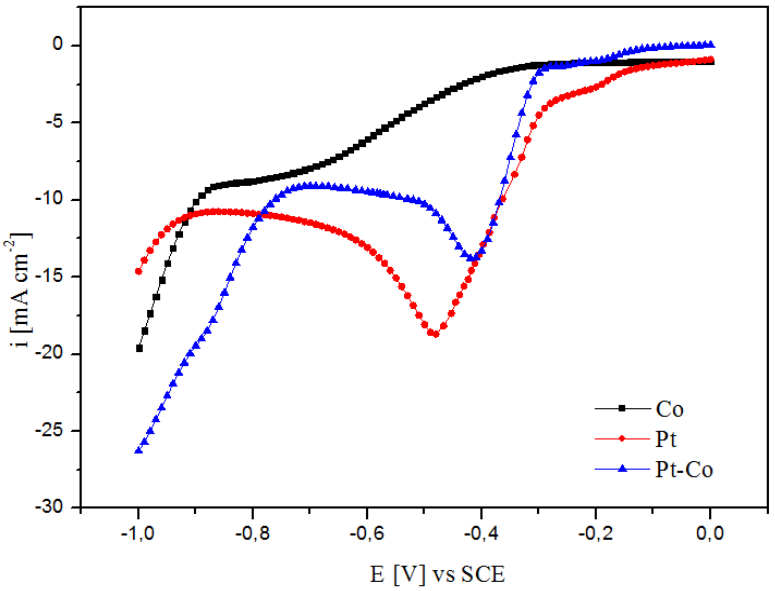

Figure 2. Linear sweep voltammograms for Co, Pt and Pt-Co (1:1) deposition process: Co - 0.1 M $CoCl_2$ solution; Pt - 5 mM K_2PtCl_4 solution; Pt-Co alloy: 5 mM K_2PtCl_4; + 5 mM $CoCl_2$ solution; scan rate 5 mV s^{-1}.

Analysing the linear voltammetric plots for Pt-Co alloy deposition, one can observe that the voltammogram shape is similar to platinum deposition. At around -0.4 V, the current density starts to decrease due to the fact the platinum or/and cobalt concentration in the diffusion layer is significantly lowered. From that point further, metallic ions diffuse to the working electrode from a higher distance and the current density becomes a function of the platinum diffusion process. HER starts faster, once the -0.7 V potential is achieved in comparison to platinum and cobalt individual depositions.

3.2. Cyclic voltammetry for Pt-Co deposition process

Valuable information is obtained from cyclic voltammograms drawn in solutions used for Pt, Co and Pt-Co alloy deposition (Fig. 3). At cathodic polarization, around -0.5 V, cobalt deposition process sets in and further, when the potential of -0.75 V is reached, a limiting current density appears. At more pronounced cathodic polarization, HER occurs simultaneously with Co deposition (Co^{2+}/Co,

$E°$ = -0.52 V vs. SCE). Consequently, in the vicinity of the metal, the electrolyte solution is alkalized, and Co^{2+} cations can precipitate to $Co(OH)_2$. In these circumstances, Co deposition may occur by $Co(OH)_2$ reduction ($Co(OH)_2/Co$, $E°$ = -0.97 V vs. SCE) [16]. At anodic polarization, around -0.5 V, a high peak assigned to cobalt oxidation process can be observed. The possibility of cobalt passivation can be as well taken into consideration, resulting species like CoOOH that come from CoOH or $Co(OH)_2$, which have been previously adsorbed onto the electrode surface [17]. Over +0.75 V, the oxygen evolution reaction takes place, simultaneously with the cobalt dissolution.

Platinum deposition starts once the 0.5 V potential is reached, towards the cathodic polarization. At more negative potentials, around -0.25 V, the HER takes place in the same time with the platinum reduction process. At -0.5 V, the current density is limited due to the fact that the diffusion of Pt^{2+} ions from the bulk of the electrolyte solution to electrode becomes rate determining step. When the potential is scanned in the anodic direction, around +0.6 V, the current density increases due to the platinum oxidation process.

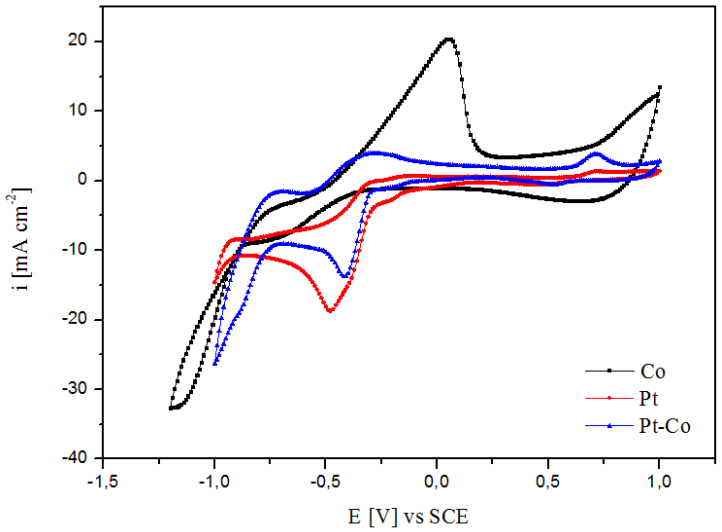

Figure 3. Cyclic voltammetry for Co, Pt and Pt-Co (1:1) deposition process: Co - 0.1 M $CoCl_2$ solution; Pt - 5 mM K_2PtCl_4; Pt-Co alloy: 5 mM K_2PtCl_4; + 5 mM $CoCl_2$ solution; scan rate 5 mV s^{-1}.

For both, Pt and Co deposition processes, the HER can be noticed in the cathodic region, the reaction being catalysed by the freshly deposited platinum and cobalt particles. For Pt-Co deposition, scanning the potential in the cathodic direction, the current density is smaller in comparison with platinum deposition in the diffusion region. The deposition of Pt-Co alloy is indicated by the cobalt oxidation peak, around -0.5 V as well as platinum oxidation around 0.6 V.

3.3. Morphology and physical properties

In order to characterize the microstructure of the prepared samples, SEM investigations have been performed and the corresponding micrographs are presented in Fig. 4. The morphology of the

obtained catalysts remains the same even if the Pt^{2+}/Co^{2+} ratio in the deposition bath is changed. The catalyst particles are uniform distributed onto the CNF surface and some regions show agglomerations.

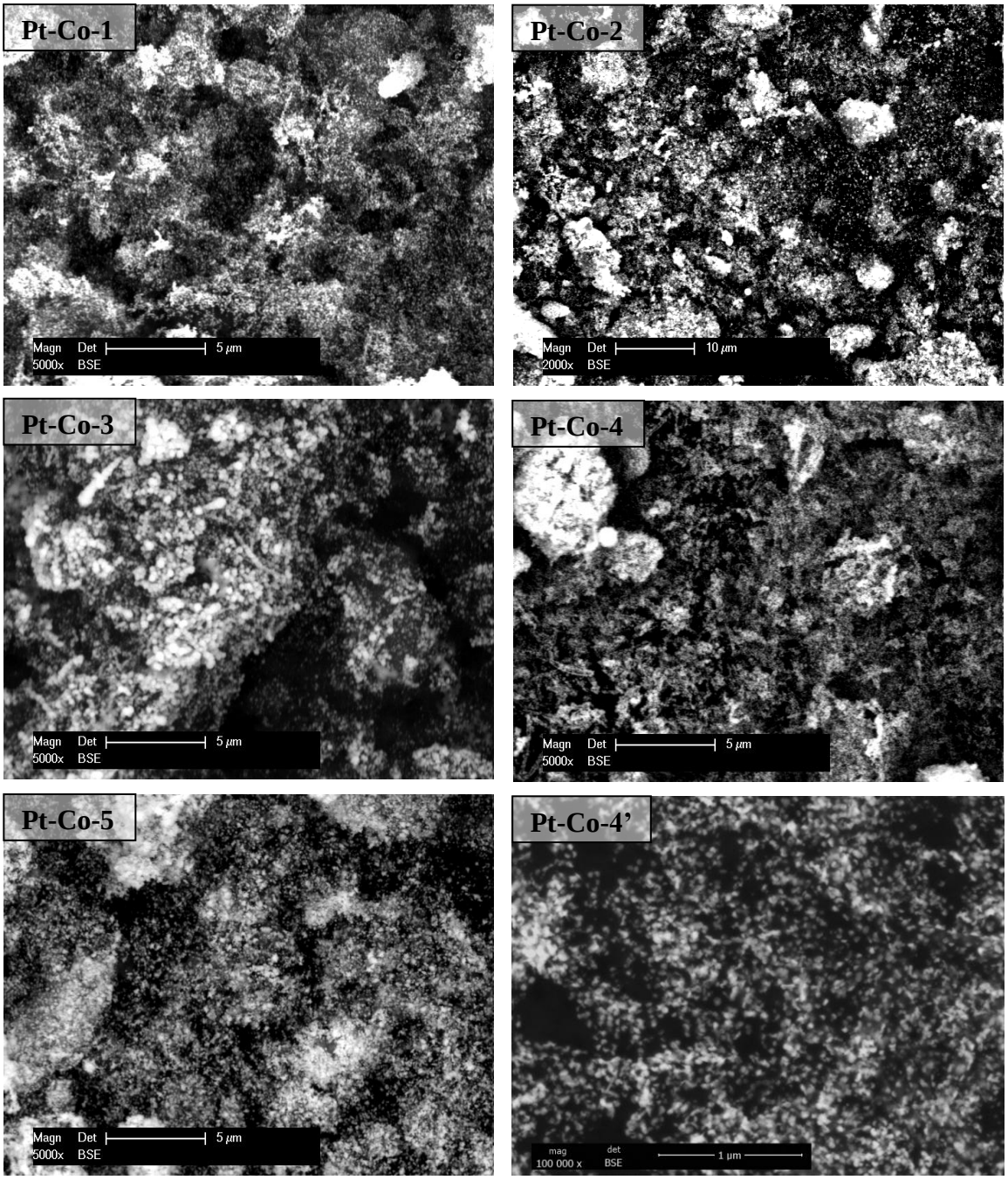

Figure 4. SEM micrographs of Pt/CNF based electrodes depending on the Pt: Co ratio in the deposition bath: Pt-Co-1 (1:0.5) – 5000x, Pt-Co-2 (1:1) – 5000x, Pt-Co-3(1:2) – 5000x, Pt-Co 4 (1:5) – 5000x, Pt-Co-4' (1:5) – 100.000 x, Pt-Co-5 (1:10) – 5000x.

The smallest particles were found for the sample Pt-Co-4 and these values are well correlated with the estimation of particles size estimated through XRD and CV method. The XRD patterns presented in Fig. 5 reveal the diffraction peaks of the Pt-Co alloy, as well as of the carbon support

material. The estimation of the average size of the crystallites was carried out using the Debby-Scherer equation (3) [6] and the obtained values are presented in Table 1:

$$d = 0.9 \frac{\lambda}{B \cos\theta} \quad (3)$$

It is important to mention that the crystallites size obtained through this method is related to the diffraction area and generally can be smaller compared to the real size of the particles. One can remark that an increase of cobalt concentration in deposition bath gives rise to a decrease in particle sizes of deposited catalyst. This aspect can be attributed to an increase of the nucleation rate induced by the increase of the overpotential at higher concentrations [18].

Moreover, increasing the deposition time and number of applied cycles respectively, leads to an increase in particles size, favouring the formation of agglomerations. Likewise, applying a higher deposition current density determines a decrease of the particles size due to the enhancement of the nucleation process. Although, this effect is limited once the current density is increased to values higher than 100 mA cm^{-2}, when the hydrogen evolution reaction is intensified, favouring the particles growth mechanism by achieving the diffusion limiting current density region.

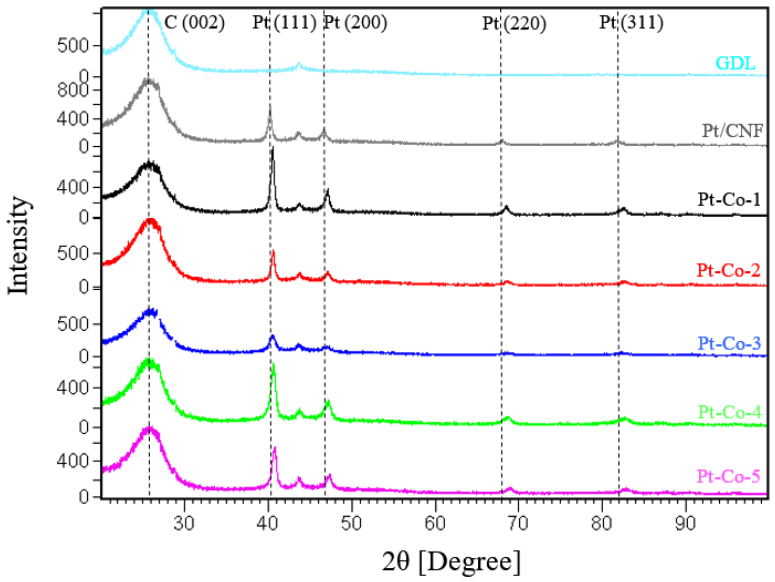

Figure 5. XRD diffractograms of the GDL, Pt and Pt-Co electrodes.

The first peak observed in the XRD diffractograms (Fig. 5), at 2θ = 26.5°, is associated with the characteristic carbon peak C (002) from the support material. For all the Pt-Co samples, a single alloy phase - $CoPt_3$ - was detected, this being present in different amounts from 45% to 60%, depending on the chemical composition of the deposition bath. The diffraction patterns of $CoPt_3$ alloy phase and pure Pt are very similar without any additional peaks. The characteristic peaks for Pt-Co alloy are slightly shifted to higher 2θ values in comparison with pure Pt diffraction peaks, this aspect indicates a contraction in the lattice constant and a high alloying degree through incorporation of smaller cobalt atoms in the platinum structure. Previous studies have revealed that by decreasing the Pt-Pt bond length, the binding energy is reduced and the catalytic activity is considerably increased [19]. In the Pt-

Co alloy structure no pure cobalt could be identified, which implies that all the cobalt atoms are incorporated in the platinum structure in order to form the $CoPt_3$ alloy.

The thermogravimetric measurements carried on Pt-Co catalyst samples are shown in Fig. 6. When a temperature of 500°C is reached, a slight mass loss can be observed, the process being assigned to combustion of organic compounds related to the GDL material. The main mass loss corresponds to the burning process of the carbon from support material (CNF and GDL) and rest mass represents the Pt-Co alloy previously deposited onto the support material surface. The possibility of Pt-Co alloy oxidation may cause a deviation in weight percent. The amount of Pt-Co alloy is strongly influenced by deposition parameters, as well as by the amount of CNF and their functionalization degree. Table 1 summarizes the catalyst amount obtained for each of the investigated sample. Moreover, it was found that the presence of transitional metals onto the CNF surface may deform the carbon lattice, causing local defects which increase the chemical reactivity and reduce the carbon oxidation temperature [20].

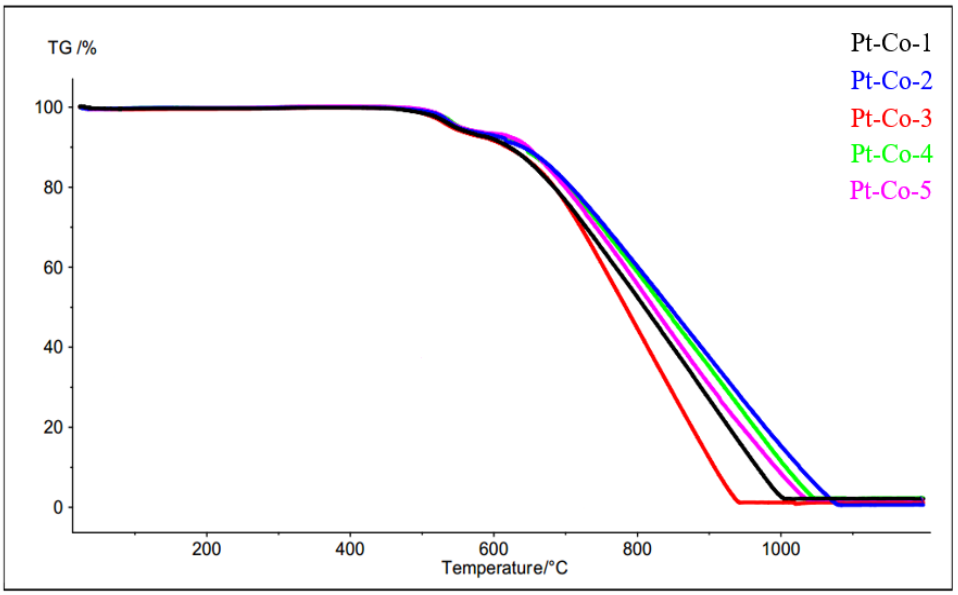

Figure 6. Thermogravimetric investigations in synthetic air atmosphere on Pt-Co electrodes.

The cyclic voltammetry can be regarded as a suitable technique for studying the electrochemical properties and reactions of the atom surface and less for volume and mass properties. The electrochemical surface area (*ECSA*) can be calculated using the cyclic voltammograms plotted in 0.5 M H_2SO_4, regarding the hydrogen adsorption/desorption region, between -0.2 V and 0.1 V, obtaining the necessary charge for the hydrogen adsorption/desorption process after the subtraction of the double layer capacity contribution [21], using equation (4):

$$ECSA = \frac{Q_{H_{des}}}{m_{Pt} \, x \, Q_{mono}} = \frac{\frac{1}{v}\int i\,(E)dE}{m_{Pt} \, x \, Q_{mono}} \qquad (4)$$

where $Q_{H_{des}}$ is the charge for hydrogen desorption (μC), m_{Pt} is the amount of Pt-Co catalyst (g), Q_{mono} is the charge necessary for the adsorption of a hydrogen monolayer on the surface of a

polycrystalline platinum electrode (210 μC cm^{-2}), *i*(*E*) is the current (μA), *v* is the scan rate (V s^{-1}), *E* is the electrode potential (V).

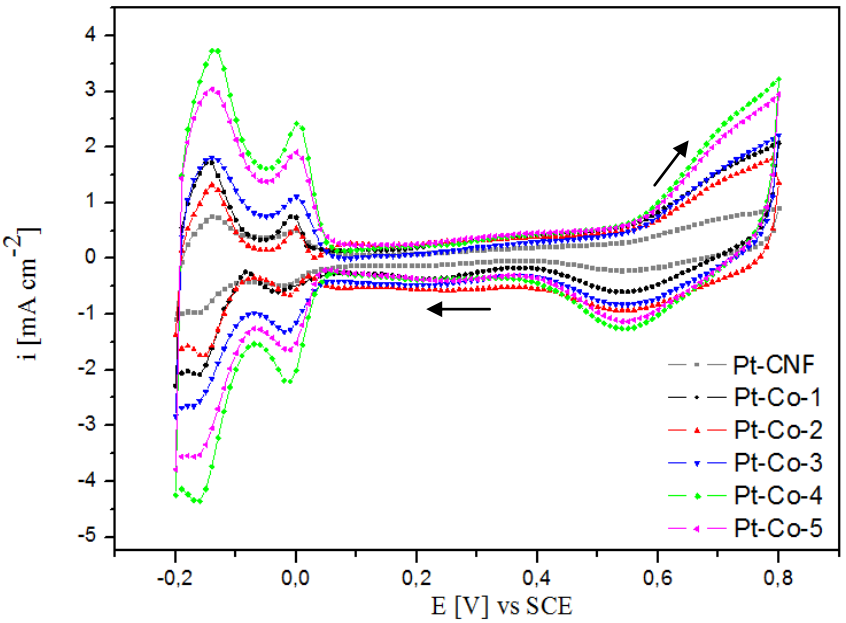

Figure 7. Cyclic voltammetry in 0.5 M H_2SO_4 on Pt-Co electrodes for *ECSA* determination, scan rate 100 mV s^{-1}.

Table 1. Chemical composition, catalyst amount, *ECSA* and particles size of Pt-Co electrodes.

Sample	Pt-Co ratio [%]				Rest mass [mg]	*ECSA* [m^2 g^{-1}]	Particles size [nm]	
	XRF		XRD				XRD	ECSA
	Pt	Co	Pt	Co				
Pt-Co-1	72	28	88	12	0.28	2.1	50	130
Pt-Co-2	69	31	87	13	0.23	2.9	32	96
Pt-Co-3	65	35	85	15	0.21	8.6	13	32
Pt-Co-4	61	39	84	16	0.18	13.5	12	20
Pt-Co-5	62	38	86	14	0.2	9.6	19	30

Fig. 7 shows the CV plots for the Pt-Co samples obtained from different deposition baths, and also, as reference, a Pt deposited sample. Two desorption/adsorption peaks can be identified at a potential value of 0.15 V (Pt 110) and 0 V (Pt 100), as well as an oxidation/reduction peak around 0.5 V. It can be remarked that sample Pt-Co-4 presents the highest current density values, which leads to higher *ECSA* (Table 1). An estimation of the deposited catalyst particles size was realized using the equation (5):

$$d = \frac{6}{\rho \, x \, ECSA} \qquad (5)$$

The particles size values obtained through this method are larger compared to those obtained through XRD method, since particles are composed of more agglomerated crystallites and also the catalyst surface might be just partially active for the studied electrochemical reactions.

4. CONCLUSIONS

In summary, this study presents a convenient method for obtaining a novel Pt-Co catalyst for electrochemical cell applications. The CNF support material has been previously treated using a clean, fast, and efficient oxygen plasma process. The applied power of 80 W for 1800 s during the functionalization treatment generates oxygen containing groups on the outer surface of CNF, which increase the wettability and promote the deposition process of the catalyst particles. The Pt-Co alloy deposition process is carried out using a pulse plating method. Varying the concentration ratio of Pt and Co in the electrodeposition bath, the chemical composition and characteristics of the obtained Pt-Co alloy particles can be adjusted. Five types of Pt-Co electrodes obtained from different composition baths have been investigated regarding their morphology, structure, and catalytic properties. The XRD analyses revealed the formation of a platinum rich alloy phase ($CoPt_3$), which exhibits enhanced catalytic activity for electrochemical processes. By increasing the cobalt concentration in the deposition bath, a higher alloying degree has been achieved. Moreover, the presented deposition process leads to reduced catalyst particle sizes of around 20 nm. The electrochemical measurements in 0.5 M H_2SO_4 indicated that Pt-Co catalysts exhibit an increased surface area of around 13 m^2 g^{-1}. This fact can be attributed to the small dimension of the alloy particles correlated with the increased surface area of the support material.

References

1. O. T. Holton and J. W. Stevenson, *Platin. Met. Rev.*, 57 (2013) 259.
2. S. H. Liu and J. R. Wu, *Int. J. Electrochem. Sci.*, 7 (2012) 8326.
3. N. Chaisubanan, K. Pruksathorn, H. Vergnes, F. Senocq and M. Hunsom, *Int. J. Electrochem. Sci.*, 11 (2016) 1012.
4. D. Morales-Acosta, D. L. Fuente, L. G. Arriaga, G. V. Gutierrez and F. J. R. Varela, *Int. J. Electrochem. Sci.*, 6 (2011) 1835.
5. A. Schenk, C. Grimmer, M. Perchthaler, S. Weinberger, B. Pichler, H. C. Scheu, A. Mautner, B. Bitschnau and V. Hacker, *J. Power Sources*, 266 (2014) 313.
6. M. Yaldagard, N. Seghatoleslami and M. Jahanshahi, *Appl. Surf. Sci.*, 315 (2014) 222.
7. N. Chaisubanan and N. Tantavichet, *J. Alloys Compd.*, 559 (2013) 69.
8. K. Hosoiri, F. Wang, S. Doi and T. Watanabe, *Mater. Trans.*, 44 (2003) 653.
9. S. C. Zignani, E. Antolini and E. R. Gonzalez, *J. Power Sources*, 182 (2008) 83.
10. K. Hyun, J. H. Lee, C. W. Yoon and Y. Kwon, *Int. J. Electrochem. Sci.*, 8 (2013) 11752.
11. L. Xiong and A. Manthiram, *Electrochim. Acta*, 50 (2005) 2323.
12. N. Kristian, Y. Yu, J. M. Lee, X. Liu and X. Wang, *Electrochim. Acta*, 56 (2010) 1000.
13. S. Woo, I. Kim, J. K. Lee, S. Bong, J. Lee and H. Kim, *Electrochim. Acta*, 56 (2011) 3036.
14. V. Chirila, G. Marginean and W. Brandl, *Surf. Coat. Technol.*, 200 (2005) 548.
15. D. R. Lide, CRC Handbook of Chemistry and Physics, *Electrochemical Series*, CRC Press, 2005.
16. J. Santos, F. Trivinho-Strixino and E. C. Pereira, *Surf. Coat. Technol.*, 205 (2010) 2585.

17. W. A. Badawy, F. M. Al-Kharafi and J. R. Al-Ajmi, *J. Appl. Electrochem*., 30 (2000) 693.
18. F. Pangnanelli, P. Altimari, M. Bellagamba, G. Granata, E. Moscardini, P. G. Schiavi and L. Toro, *Electrochim. Acta*, 155 (2015) 228.
19. Z. Yan, M. Wang, B. Huang, R. Liu and J. Zhao, *Int. J. Electrochem. Sci.*, 8 (2013) 149.
20. R. Brukh, O. Sae-Khow and S. Mitra, *Chem. Phys. Lett.*, 459 (2008) 149 .
21. M. Lukaszewski, M. Soszko and A. Czerwinski, *Int. J. Electrochem. Sci.*, 11 (2016) 4442.